

Syracuse University

SURFACE

Physics

College of Arts and Sciences

12-19-2000

Phase Diagram of Three-Dimensional Dynamical Triangulations with a Boundary

Simon Catterall
Syracuse University

Simeon Warner
Syracuse University

Ray Renken
University of Central Florida

Follow this and additional works at: <https://surface.syr.edu/phy>



Part of the [Physics Commons](#)

Recommended Citation

Catterall, Simon; Warner, Simeon; and Renken, Ray, "Phase Diagram of Three-Dimensional Dynamical Triangulations with a Boundary" (2000). *Physics*. 477.
<https://surface.syr.edu/phy/477>

This Article is brought to you for free and open access by the College of Arts and Sciences at SURFACE. It has been accepted for inclusion in Physics by an authorized administrator of SURFACE. For more information, please contact surface@syr.edu.

Phase diagram of three-dimensional dynamical triangulations with a boundary

Simeon Warner*, Simon Catterall*, Ray Renken†

* Department of Physics, Syracuse University, Syracuse, NY 13210, USA

† Department of Physics, University of Central Florida, Orlando, FL 32816, USA

Abstract

We use Monte Carlo simulation to study the phase diagram of three-dimensional dynamical triangulations with a boundary. Three phases are identified and characterized. One of these phases is a new, boundary dominated phase; a simple argument is presented to explain its existence. First-order transitions are shown to occur along the critical lines separating phases.

Dynamical triangulations with a boundary term

Dynamical triangulation models arise from simplicial discretizations of continuous Riemannian manifolds. A manifold is approximated by glueing together a set of equilateral simplices with fixed edgelengths. This glueing ensures that each face is shared by exactly two distinct simplices – the resultant simplicial lattice is called a triangulation. In the context of Euclidean quantum gravity it is natural to consider a weighted sum of all possible triangulations as a candidate for a regularized path integral over metrics. Physically distinct metrics correspond to inequivalent simplicial triangulations. This prescription has been shown to be very successful in two-dimensions (see, for example, [2]).

Most analytic studies and almost all numerical work done so far has been restricted to compact manifolds like the sphere. In this paper we develop techniques that allow us to extend numerical studies to simplicial manifolds with boundaries. Specifically, we study the 3-disk created by inserting an S^2 boundary into a triangulation of the sphere S^3 . This allows us to compute an object which is the simplicial equivalent of the ‘wavefunction of the Universe’ [9]:

$$\psi [h] = \int Dg e^{-S(g)} \tag{1}$$

The functional integral over 3-metrics g is restricted to those with 2-metric h on the boundary. The simplicial analog is simply

$$\psi(T_2) = \sum_{T_3} e^{-S_L(T_3)} \quad (2)$$

Thus the probability amplitude for finding a particular 2-triangulation T_2 is obtained by counting (with some weight) all 3-triangulations T_3 which contain T_2 as their boundary. A natural lattice action S_L can be derived from the continuum action by straightforward techniques [10]. It contains both the usual Regge curvature piece familiar from compact triangulations together with a boundary term. The boundary term arises from discretization of the extrinsic curvature of the boundary embedded in the bulk. In three-dimensions the curvature is localized on links. If L_M denotes the set of links in the bulk of the 3-triangulation (excluding the boundary) and $L_{\partial M}$ those in the boundary the action can be written

$$S_L = \kappa_1 \left(\sum_{h \in L_M} (2\pi - \alpha n_h) + \sum_{h \in L_{\partial M}} (\pi - \alpha n_h) \right) \quad (3)$$

The quantity $\alpha = \arccos(1/3)$ and n_h is the number of simplices sharing the link (hinge) h . Typically S_L will also contain a bulk cosmological constant that can be used to tune the simulation volume. The resultant action can be rewritten in the form

$$S_b = -\kappa_0 N_0 + \kappa_3 N_3 + \kappa_b N_2^b \quad (4)$$

where N_2^b is the area of the boundary. Here, κ_3 is used to tune the volume of the system. We are thus left with a two-dimensional phase space parameterized by κ_0 and κ_b conjugate to the number of vertices and the number of boundary triangles. It is trivial to generalize this to, for example, four-dimensions. The partition function for the system is then

$$Z = \sum_T e^{-S_b} \quad (5)$$

where the sum is over triangulations, T .

Various other extended phase diagrams have been studied for three-dimensional dynamical triangulations including adding spin matter [13, 5], adding gauge matter [12, 4], and adding a measure term [14]. Much of this work was motivated by the desire to find a continuous phase transition. No such transitions have been found.

Simulation

Our simulation algorithm is an extension of the algorithm for compact manifolds in arbitrary dimension described by Catterall [7]. Consider the environment of any vertex in a D -triangulation

— it is composed of simplices making up a trivial D -ball. The boundary of this D -ball is just the sphere $S^{(D-1)}$. A boundary with the topology of $S^{(D-1)}$ can thus be created in the original triangulation by removing these simplices. If the original triangulation corresponded to the sphere S^D the topology of the new triangulation is that of a D -disk.

In practice we simulate a compact manifold with one ‘special’ vertex. This vertex and all the simplices sharing it are ignored during any measurement. In this way every triangulation of our marked sphere S^D is in one-to-one correspondence with a triangulation of the D -disk. Notice that the usual compact manifold moves applied to all simplices (including those sharing the special vertex) will in general change the boundary of the D -disk. Indeed these moves are ergodic with respect to the boundary. Furthermore, the proof that these moves satisfy a detailed balance relation goes through just as for the compact case. The one extra restriction is simple — one must never delete the special vertex. With this trick we can trivially extend our compact codes to the situation in which a $S^{(D-1)}$ boundary has been added. We are merely simulating a compact lattice with an action which singles out a special vertex and its neighbour simplices. This contrasts with the set of additional boundary moves used by Adi *et al* [1] for simulations in two-dimensions.

Measurements do not include the special vertex or any simplices connected to it. For example, the number of D -simplices in the system with boundary is the number of D -simplices in the whole simulation minus the number of D -simplices sharing the special vertex. The size of the boundary is simply the number of D -simplices sharing the special vertex.

We have used the Metropolis Monte Carlo [11] scheme with usual update rule:

$$p(\text{accept move}) = \min\{e^{-\Delta S_b}, 1\} \tag{6}$$

and in this way we explore the space of unlabeled triangulations with the action S_b (equation 4 for three-dimensions).

Checks in two-dimensions

In two dimensions we tested our simulation code at small volumes by comparing with hand calculated amplitudes for small disks. We label disk configurations by the number of triangles and the boundary length: (N_2, N_1^b) . We calculated the ratios of amplitudes for disks (1,1):(2,4):(3,3):(3,5) to be 1:1.5:1:3. Our simulation gave 1.01:1.52:1:3.04 from a sample of 1 million disks with volume 1–3. This test was extended up to volume 5 disks, also showing good agreement.

We also tested our simulation code by comparing results for two-dimensions of Adi *et al* [1]. All our results agree within the statistical errors. Table 1 shows a comparison of the results for a selection of lattice sizes.

N_2	$\langle N_1^b \rangle$ (Adi <i>et al</i>)	$\langle N_1^b \rangle$ (this work)
50	39.83(5)	39.88(4)
100	78.05(5)	78.09(4)
200	154.54(6)	154.57(6)
400	307.62(8)	307.53(8)
800	613.4(1)	613.4(1)
1600	1225.1(1)	1225.1(2)
3200	2448.7(2)	2448.8(3)
6400	4895.6(3)	4895.4(13)

Table 1: Estimates of $\langle N_1^b \rangle$, the expectation value of the boundary size (length), for two-dimensional manifolds of various sizes from Adi *et al* [1], and from this work.

Phase diagram

We performed a set of simulations in three-dimensions with action of equation 4. In all runs κ_3 was used to tune the nominal system volume, N_3 , to 2000 for each given κ_0 and κ_b .

In three-dimensions there are just 4 types of move: vertex insertion, vertex deletion and exchange of a link with a face (two moves: link to face or face to link). Where these moves take place on sections of the triangulation involving the special vertex we take care to count changes in the numbers of simplices inside and outside of the boundary but otherwise the moves are the same as for the bulk. Series of runs varying either κ_0 or κ_b were made and the vertex susceptibility used to search for phase transitions. We define the vertex susceptibility, χ , to be normalized with respect to the number of 3-simplices:

$$\chi = \frac{1}{N_3} (\langle N_0^2 \rangle - \langle N_0 \rangle^2) \quad (7)$$

The points shown in figure 1 are taken from the positions of peaks in the vertex susceptibility.

In figure 1 there are three phases which we characterize as: phase 1 - crumpled, minimal boundary; phase 2 - branched-polymer, minimal boundary; and phase 3 - boundary dominated. In phases 1 and 2 the boundary is simply 4 triangles (2-simplices) connected to form a tetrahedral hole. The system is essentially like a compact manifold with one marked 3-simplex — the tetrahedral hole. In phase 3 the boundary is large — typically a substantial fraction of the bulk volume.

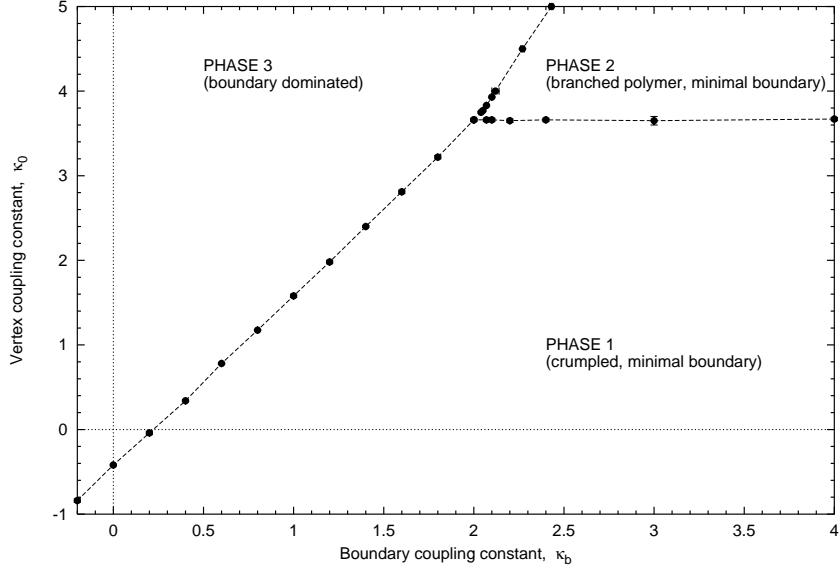


Figure 1: Phase diagram for 3-dimensional dynamical triangulation with a boundary. All points have error bars in either κ_b or κ_0 , most cannot be seen because they are smaller than the symbols. Nominal simulation volume, $N_3 = 2000$.

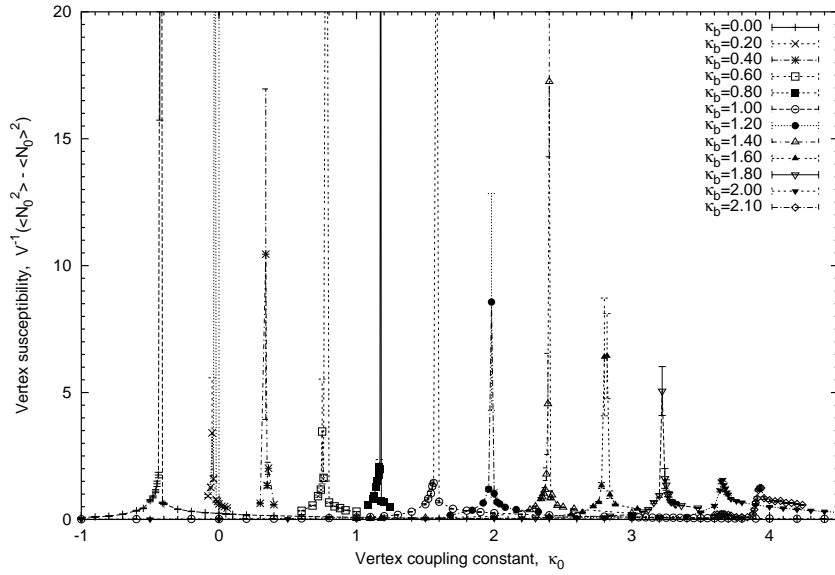


Figure 2: Sample of vertex susceptibility data for different values of the boundary coupling constant, κ_b .

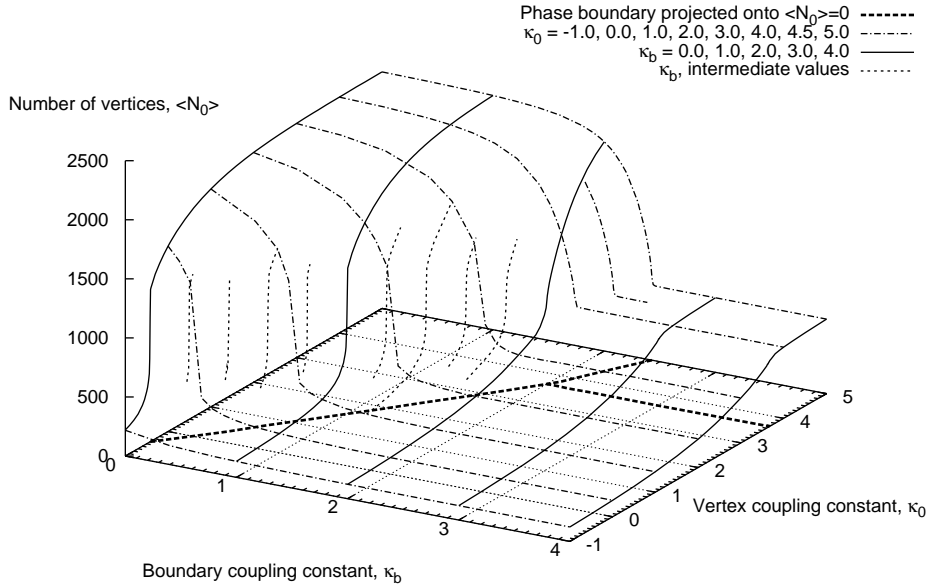


Figure 3: Number of vertices, $\langle N_0 \rangle$, as a function of κ_0 and κ_b . Nominal simulation volume, $N_3 = 2000$. Note that we see three distinct areas with different values of $\langle N_0 \rangle$: the boundary dominated phase (small κ_b , large κ_0) with large $\langle N_0 \rangle$, the crumpled phase (small κ_0) with small $\langle N_0 \rangle$, and the branched-polymer phase (large κ_b and κ_0) with intermediate $\langle N_0 \rangle$.

Simple argument for boundary dominated phase

Here we argue that the boundary dominated phase can be explained by considering an effective action written in terms of the boundary size. We show that in certain circumstances a large boundary will decrease this action. Otherwise one of the minimal boundary phases will be favored.

Consider the action:

$$S_b = -k_0 N_0 + k_b N_2^b \quad (8)$$

We ignore the volume term as this is kept fixed during the simulation. If we note that the boundary is itself a 2-sphere then we know that:

$$N_2^b = 2(N_0^b - 2) \quad (9)$$

and

$$N_0 = N_0^b + N_0^i \quad (10)$$

where N_0 is the number of vertices, N_0^b is the number of vertices on the boundary, N_0^i is the number of internal vertices, and N_2^b is the number of 2-simplices (triangles) on the boundary. We may thus rewrite the action:

$$S_b = -\kappa_0 N_0^i + (2\kappa_b - \kappa_0) N_0^b \quad (11)$$

If we now consider N_0^i fixed and note that the number of manifolds with boundary size N_2^b is governed by an exponential factor $e^{\kappa_b^c N_2^b} = e^{2\kappa_b^c N_0^b}$, where κ_b^c is a new constant, we may then write an effective action for the number of boundary vertices:

$$S_{eff} \approx (-\kappa_0 + 2(\kappa_b - \kappa_b^c)) N_0^b \quad (12)$$

The presence of small or large boundaries is then determined by the sign of this action. We thus expect the phase transition at $\kappa_0 = 2(\kappa_b - \kappa_b^c)$ which is in good agreement with what we see.

Order of transitions

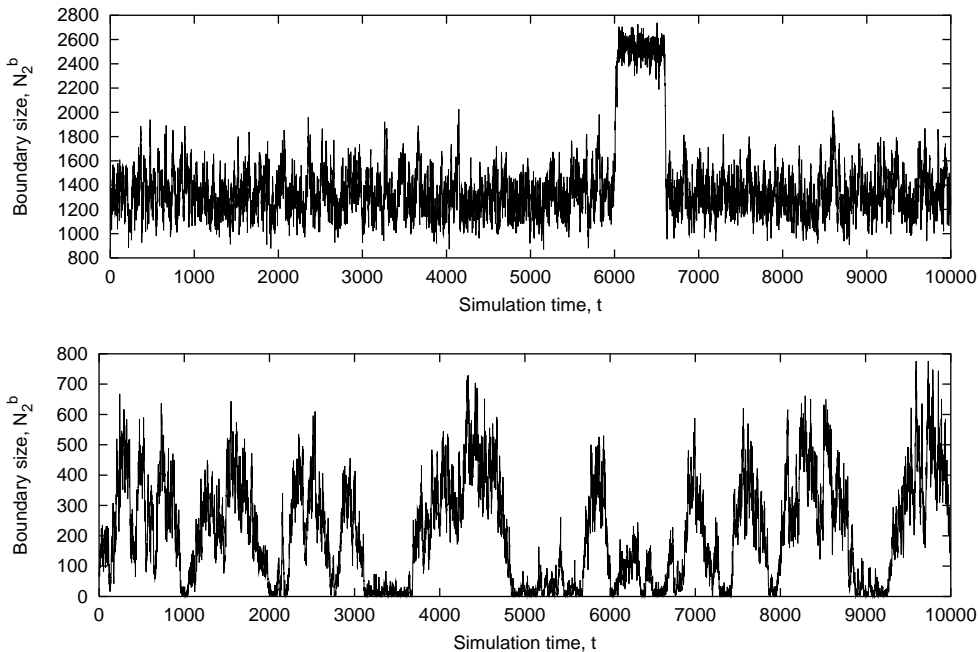


Figure 4: Time series showing the boundary size (N_2^b) during simulation. The upper plot is at the transition between the crumpled and boundary dominated phases ($k_0 = -0.423$, $k_b = 0$). The lower plot is at the transition between the branched-polymer and boundary dominated phases ($k_0 = 5$, $k_b = 2.43$). Nominal simulation volume, $N_3 = 2000$, and time is in units of $100N_3$ attempted updates.

Simulations of compact manifolds in three and four-dimensions are known to have a first-order phase transition between crumpled and branched polymer phases (3d [3], 4d [6, 8]). Our Monte Carlo time series show strong bistability on all three phase boundaries (see figure 4). We take this to indicate that all three phase transitions are first-order.

Concluding remarks

We have demonstrated an arbitrary dimension algorithm for simulating dynamical triangulations with a boundary. This has been tested against known results in two-dimensions and used to map the phase diagram in three-dimensions.

We have identified three phases in three-dimensional dynamical triangulations with a boundary and mapped the boundaries within the range of couplings $-1 < \kappa_0 < 5$ and $-0.5 < \kappa_b < 4$. The observed phases include the crumpled and branched-polymer phases seen in triangulations of compact manifolds, and also a new, boundary dominated phase. The existence of this phase, and the shape of the phase boundary on the κ_0 - κ_b phase diagram, is predicted by a simple argument. Obvious bistability in the time series at the phase transitions indicates that all transitions within the range of couplings studied are first-order.

Acknowledgments

Simon Catterall was supported in part by DOE grant DE-FG02-85ER40237. Ray Renken was supported in part by NSF grant PHY-9503371.

References

- [1] E Adi, M Hasenbusch, M Marcu, E Pazy, K Pinn and S Solomon. Monte carlo simulation of 2-d quantum gravity as open dynamically triangulated random surfaces. *XXX archive hep-lat/9310016* (1993).
- [2] J Ambjorn. Quantization of geometry. *XXX archive hep-th/9411179* (1994).
- [3] J Ambjorn, D V Boulatov, A Krzywicki and S Varsted. The vacuum in three-dimenaional simplicial quantum gravity. *Physiscs Letters B*, **276** 432–436 (1992).

- [4] J Ambjorn, J Jurkiewicz, S Bilke, Z Burda and B Petersson. z_2 gauge matter coupled to 4-d simplicial quantum gravity. *Modern Physics Letters A*, **9** 2527–2541 (1994).
- [5] J Ambjorn, C Kristjansen, Z Burda and J Jurkiewicz. *Nuclear Physics B Proc. Suppl.*, 771–(1993).
- [6] P Bialas, Z Burda, A Krzywicki and B Petersson. Focusing on the fixed point of 4d simplicial gravity. *Nuclear Physics B*, **472** 293–308 (1996). Also *XXX archive* [hep-lat/9601024](#).
- [7] S Catterall. Simulations of dynamically triangulated gravity - an algorithm for arbitrary dimension. *Computer Physics Communications*, **87** 409–415 (1995).
- [8] B de Bakker. Further evidence that the transition of 4d dynamical triangulation is 1st order. *Physics Letters B*, **389** 238–242 (1996). Also *XXX archive* [hep-lat/9603024](#).
- [9] J B Hartle and S W Hawking. Wave function of the universe. *Physical Review D*, **12** 2960–2975 (1983).
- [10] J B Hartle and R Sorkin. Boundary terms in the action for the regge calculus. *General Relativity and Gravity*, **13** 541–549 (1981).
- [11] Nicholas Metropolis, Arianna W Rosenbluth, Marshall N Rosenbluth, Augusta H Teller and Edward Teller. Equation of state calculations by fast computing machines. *The Journal of Chemical Physics*, **21** (1953).
- [12] Ray L Renken, Simon M Catterall and John B Kogut. Three dimensional quantum gravity coupled to ising matter. *Nuclear Physics B*, **389** 601–610 (1993).
- [13] Ray L Renken, Simon M Catterall and John B Kogut. Three-dimensional quantum gravity coupled to gauge fields. *Nuclear Physics B*, **422** 677–689 (1994).
- [14] Ray L Renken, Simon M Catterall and John B Kogut. Phase structure of dynamical triangulation models in three dimensions. *XXX archive* [hep-lat/9712011](#) (1997).